Smart Materials and Structures

PAPER

Pop-up cookie molds: self-folding elastomer sheets using thermal expansion of embedded air chambers

To cite this article: Junghan Kwon *et al* 2021 *Smart Mater. Struct.* **30** 115013

Smart Mater. Struct. **30** (2021) 115013 (12pp) https://doi.org/10.1088/1361-665X/ac2919

Pop-up cookie molds: self-folding elastomer sheets using thermal expansion of embedded air chambers

Junghan Kwon, Myungsun Park, Jaeyoun Choi and Yong-Lae Park*

Department of Mechanical Engineering, Institute of Advanced Machines and Design (IAMD), Institute of Engineering Research, Seoul National University, Seoul, Republic of Korea

E-mail: ylpark@snu.ac.kr

Received 31 March 2021, revised 18 June 2021
Accepted for publication 21 September 2021
Published 5 October 2021

Abstract

Self-folding is a promising concept in the fields of smart materials and robotics, which allows self-assembly and multi-functionality. Although there have been approaches to realize self-folding mechanisms using different techniques, and their practical applications are not sufficiently investigated. Here, we propose untethered, self-folding polymer structures with embedded air chambers, which easily transform two-dimensional flat shapes into preprogrammed three-dimensional (3D) shapes when heat energy is transferred into the structures resulting in thermal expansion of the air chambers. This mechanism is particularly useful for casting materials that require shape and phase changes simultaneously if the proposed structures are used as molds. As a practical application, we present pop-up cookie molds that can bake 3D-shaped cookies from flat cookie dough. Analytical modelings based on the ideal gas law, the principle of minimum potential energy, and the lumped capacitance method for heat transfer are established and experimentally validated using prototypes. These provide a prediction of the structure's bending curvature during the baking process. Furthermore, other target shapes, including bending, twisting, and their combinations, are also achieved by configuring various chamber designs. Finally, practical prototypes with more complex shapes are proposed, and their performances are demonstrated.

Supplementary material for this article is available online

Keywords: self-folding, preprogrammed transformation, soft actuators, thermal expansion, pop-up fabrication

(Some figures may appear in colour only in the online journal)

1. Introduction

According to the recent trend of food culture, the visual appearance of food is as essential as the taste and the flavor for the attention of the consumers and the increased sales of the products [1, 2]. For example, bakers often prefer three-dimensional (3D) shapes to simple flat shapes when they make cookies with unique shapes and decorations. However, fabricating food products with complex shapes requires professional skills and experiences. It is also difficult to control the quality during mass production, resulting in cost increase and low productivity. In the automated food industry, manufacturers sometimes simplify the food shapes despite their importance in sales due to various reasons, such as efficiency, workload, and quality, which are critical to fast and repetitive operations. This leads us to think about how to manufacture low-cost and high-productive food products that are still attractive in appearance.

Innovations in digital manufacturing and robotics have recently been introduced in the food industry. There has been

* Author to whom any correspondence should be addressed.

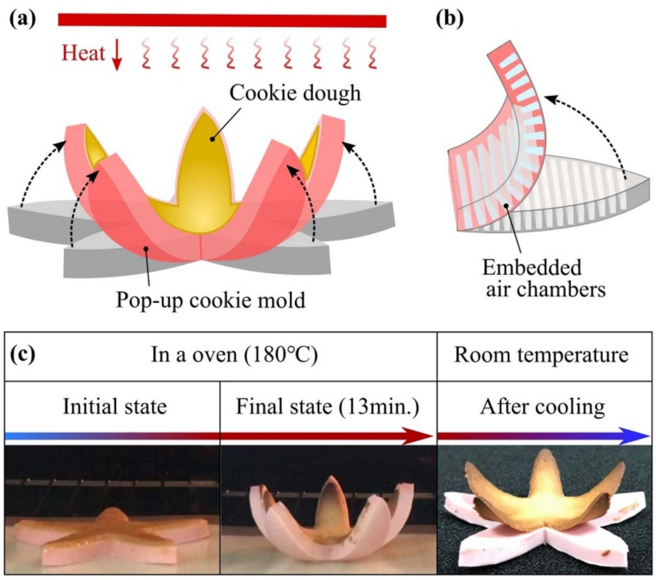

Figure 1. Pop-up cookie mold for baking 3D cookies. (a) Conceptual illustration of transformation mechanism. (b) Self-folding by thermal expansion of the embedded air chambers. (c) Demonstration of baking a flower-shaped cookie.

a study that proposed use of a humanoid robot to bake cookies to reduce the workload of human workers and to improve the efficiency [3]; however, the system was able to produce cookies with only flat and simple shapes. Another attempt is food printing based on additive manufacturing techniques [4, 5]. Some studies have proposed processes of baking cookies using food printing that can extrude cookie dough with specific designs [6–8]. This method not only provides various shapes and colors but also allows to control the proportion of nutrients and the quality during repeated operations. However, the shapes of cookies are still limited to flat shapes because the 3D cookie dough made in advance easily flowed down during the baking process [6]. The 4D-printing technology has also been introduced, which adds an additional dimension of time to the 3D-printed objects [9, 10]. In this method, a structure transforms into the preprogrammed shape triggered by certain conditions, such as temperature and light [11, 12]. It has been shown that flat structures made of edible materials could transform to predefined 3D shapes by water absorption [13]. This technique simplifies the initial form of the product to a small package with low shipping cost, but the availability of edible materials for self-folding is limited.

The concept of this work, pop-up cookie molds, originated from a traditional method of baking cookies, which includes a casting process that allows for quick and easy reproduction of a structure with the same shape and pattern in a short period of time. In this work, we incorporate s self-folding function into cookie molds, as illustrated in figure 1(a). During the baking process in an oven, the molds can change their shapes and consequently transform the shapes of the cookie dough on the molds into 3D structures when baking is done.

To be practical, self-folding cookie molds should meet the following requirements: (a) deformation to the target 3D shape from a 2D design, (b) supporting the weight of the cookie dough during transformation, (c) maintaining desired response time to prevent the cookie dough from flowing or breaking, and (d) returning to the original shape when cooled down to be reusable. In addition, the materials of the mold must (e) withstand the baking temperature up to 180 °C, and (f) be chemically safe for food. Finally, they should be (g) easy to design and fabricate.

There have been technologies to realize folding mechanisms activated by pneumatic [14–19], heat [20–29], light [30–33], electromagnetic fields [34, 35], and chemical reactions [36, 37]. In this study, we focus on simple thermal expansion of air by heat energy because baking requires the environment of a high temperature (i.e. a baking oven). Although composites containing shape-memory-alloys (SMAs) [38, 39] and thermoplastic shape-memory-polymers (SMPs) [24, 27] can be combined with heat too, precise placement of embedding SMA wires in the composites is difficult for fabrication. Moreover, SMP materials cannot withstand high baking temperature.

To address these issues, we propose untethered, self-folding polymer molds that can be deformed by thermal expansion of the embedded air chambers in response to the external heat energy, as shown in figure 1(b). The mold can be made of a single polymer material without special or additional components, and it can transform from a flat shape to a preprogrammed 3D shapes, as shown in figure 1(c). In this paper, we first analyze the shape transformation mechanism of the cookie mold through analytical modeling based on the ideal gas law, the principle of minimum potential energy, and the lumped capacitance method for heat transfer. We then evaluate our models through experimental characterization using prototypes. Lastly, we present designs with different chamber arrangements that transform into different 3D shapes and demonstrate practical prototypes of the pop-up cookie molds.

2. Design and fabrication

2.1. Design and operating principle

A simple way to inflate a balloon is injection of compressed air through the inlet, which increases the internal pressure and the volume, as shown in figure 2(a). Based on the concept of a thermodynamic system [40], it is an open system where the surface of the balloon is the control surface, the internal volume is the control volume, the inflow of the compressed air is the mass flow from the outside of the system, and the air temperature is assumed to be constant. Figure 2(b) illustrates a typical design of a PneuNet (i.e., Pneumatic network) bending actuator [14] using this approach, which drives the actuator by inflating the embedded air-chamber networks through the air inlet. A strain-limiting layer on one side of the actuator makes the chambers expand towards the opposite side, resulting in a bending motion.

The balloon can also be inflated by applying heat energy to increase the internal temperature if the inlet is closed. It increases the internal pressure and the volume, as illustrated in figure 2(c). It is a closed system with constant internal mass

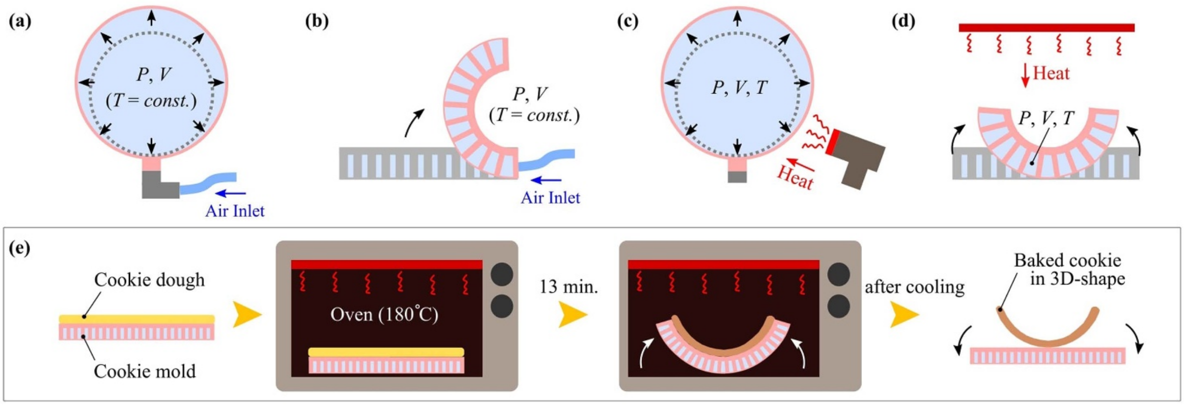

Figure 2. Design and operating principle. (a) Inflation of a balloon by external air input. (b) The PneuNets bending actuator pressurized by external air input. (c) Inflation of a balloon by thermal expansion of internal air. (d) The self-folding polymer sheet pressurized by thermal expansion of internal air. (e) Cookie baking process with the proposed pop-up cookie mold.

without flow across the boundary. Instead, the heat energy can be transmitted through the boundary resulting in a state change of the system. In this sense, we propose a polymer sheet with embedded air chambers similar to the design of a PneuNet actuator; however, each chamber is closed by the surrounding polymer material without an air inlet, as shown in figure 2(d), and the performance is dependent on the material. As the air temperature inside the chamber increases due to the external heat energy, the internal pressure and the volume also increase, and the sheet consequently transforms to an arc shape.

Using the proposed design, we developed a pop-up cookie mold with a function of self-folding to transform the shape of the cookie dough during baking and finally to make a 3D-shaped cookie. Figure 2(e) shows the process of baking a 3D-shaped cookie. First, mixed cookie dough on the flat mold is placed in a preheated oven of 180 °C. As the temperature inside the air chambers in the mold gradually increases, the mold and the cookie dough simultaneously start to transform into a bent shape. The mold continues to deform until it reaches the target shape and then maintains its shape while the dough is fully baked for 13 min of baking time. When the baked cookie is taken out of the oven and left at room temperature, the cookie maintains the curvature, while the cookie mold returns to its original flat shape. It is because the internal volume of the embedded chamber decreases when it cools down.

2.2. Fabrication process

Figure 3 shows the fabrication process of the proposed cookie mold made of a polymer sheet with embedded air chambers, similar to that of PneuNet actuators [14, 41]; however, there is no air inlet and interconnections between the chambers. The top layer of the structure was designed to be thicker than the bottom one so that it could be stiffer and play a role of a strain-limiting layer.

Two separate molds for casting the parts of the polymer sheet were first designed and fabricated using a 3D-printer (Objet30 Prime, Stratasys). Then, the food-grade silicone elastomer (Smooth-Sil 940, Smooth-On Inc.) was mixed, poured into each mold, and cured for 24 h. The cured top

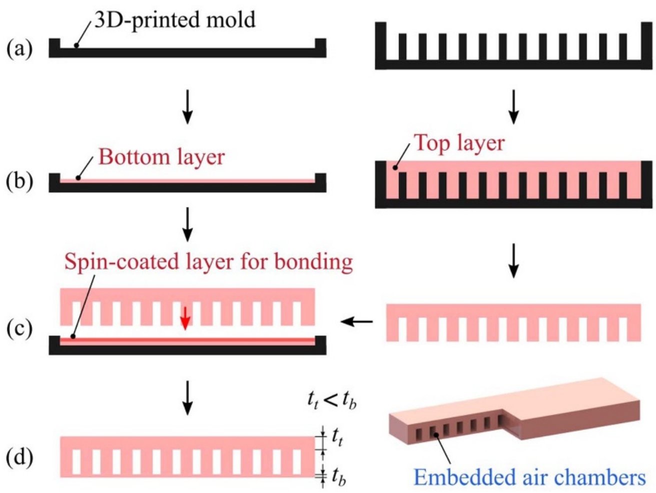

Figure 3. Fabrication process. (a) Design and fabricate the 3D-printed molds. (b) Pour uncured silicone elastomer into the molds and cure them, (c) Attach the top silicone layer already cured on the spin-coated bottom layer. (d) Completed structure with embedded air chambers.

and bottom layers were then bonded by spin-coating the same uncured silicone between the layers [42, 43]. Finally, the assembled structure was cured for an additional 24 h. In our study, we decided to cure the polymer material at room temperature to prevent formation of small air bubbles and unwanted deformation of the structure during curing and also to provide sufficient time for bonding of two cured layers through cross-linking. Figure 3(d) shows the complete polymer sheet for the 3D cookie mold with embedded air chambers biased towards the bottom of the structure, enabling upward bending of the mold.

3. Analytical modeling

3.1. Geometric assumptions

Analytical models were developed to predict the transformed shape of the proposed structure. Figures 4(a) and (b) present

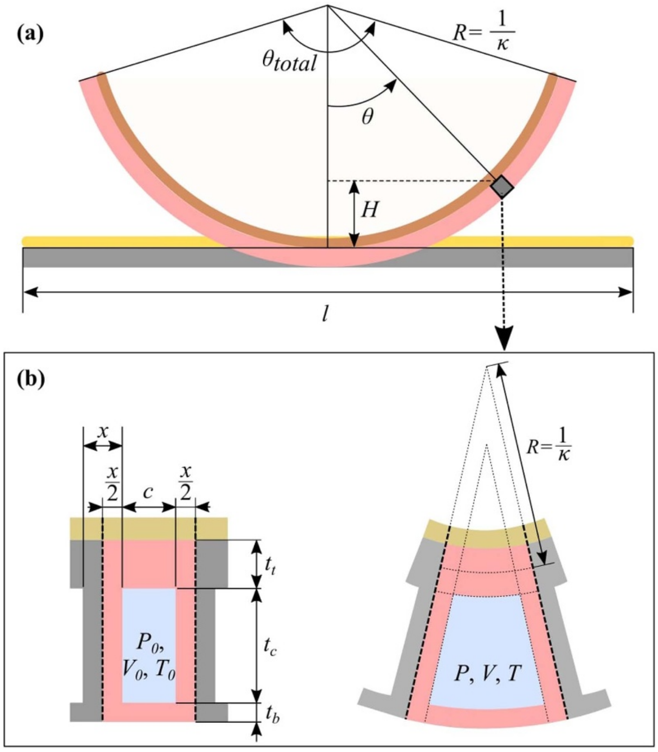

Figure 4. (a) Schematic diagram of the polymer sheet with the embedded air chambers for the cookie mold. (b) Unit chamber in an undeformed state and a deformed state.

the schematic diagrams of the polymer sheet with embedded air chambers and a unit segment of the sheet, respectively. In the undeformed state, each air chamber has the dimensions of length c, interval x, width w, and thickness t_c. The chamber is enclosed by the top layer with thickness t_t and the bottom layer with thickness t_b. As a strain-limiting layer, the top layer is designed to be thicker than the bottom layer.

The assumption of our model originated from the model of a Pneu-Net actuator, which has an array of elongated air chambers. It is also assumed that the actuator has a sufficient number of air chambers. When the sheet inflates, it is assumed that the sheet deforms to a circular arc with the bend radius R and the corresponding curvature $\kappa = 1/R$. If the sheet is designed with only one or a small number of the air chambers, our model may result in discrepancy with actual deformation, such as uniformed bending depending on the ratio of the chamber length and the chamber interval (i.e. the sidewall thickness) which is not the case of our study.

3.2. The ideal gas law

As mentioned in the previous section, PneNet actuators are operated by external air pressure, which induces the changes in volume inside the air chambers, while the temperature is assumed to be constant according to the analytical models [44, 45]. On the other hand, our approach utilizes the change in temperature by external heat energy. Temperature increase causes the change in the internal pressure and consequently the volume of each air chamber. The relation can be expressed by the ideal gas law as:

$$P_{abs}V = nRT, \tag{1}$$

where P_{abs} is the absolute pressure inside the chamber, V is the chamber volume, T is the Kelvin temperature inside the chamber, n is the number of moles of gas, and R is the ideal gas constant. Since each air chamber is a closed system surrounded by the polymer layers and the walls, $nR = P_0V_0/T_0$ is obtained from the initial conditions of P_0, V_0, and T_0, which are the atmospheric pressure, the initial chamber volume, and the room temperature, respectively. By substituting the initial conditions in equation (1), the gage pressure P can be obtained as:

$$P = \left(\frac{P_0V_0}{T_0}\right)\cdot\frac{T}{V} - P_0. \tag{2}$$

3.3. Principle of minimum potential energy

The total potential energy, Π at the deformed shape is expressed as:

$$\Pi = N\cdot\left(-\int PdV + U_t + U_b + U_h\right) + U_g, \tag{3}$$

where $-\int PdV$ is the work done by the pressure for a unit chamber; U_t, U_b, and U_h are the elastic potential energies stored in the top layer, in the bottom layer, and in the side walls of the unit chamber, respectively; N is the total number of the chambers inside the mold; and U_g is the gravitational potential energy.

The air chamber volume V was approximated from the deformed geometry, as shown in figure 4(b), which is:

$$V(\kappa) = \left(ct_c + \frac{1}{2}t_c^2c\kappa\right)\cdot w. \tag{4}$$

In the segment of the top layer, we assume that the top layer stores the bending energy while the stretching energy is neglected due to its large thickness. Then, the elastic potential energy of the top layer U_t is provided by:

$$U_t(\kappa) = \frac{1}{2}D\kappa^2\cdot(c+x) \tag{5}$$

where $D = E\cdot\left(wt_t^3/12\right)$ is the flexural rigidity of the top layer, and E is the Young's modulus of the polymer material.

The stretching energy is dominant at the bottom layer while the bending energy is negligible due to its thin thickness. Assuming that the polymer material is an incompressible Neo-Hookean material under uniaxial tension, the strain energy applied to the bottom layer U_b is obtained as:

$$U_b(\kappa) = \frac{E}{6}\cdot\left(\lambda_1^2+\lambda_2^2+\lambda_3^2-3\right)\cdot ct_bw, \tag{6}$$

where $\lambda_1 = (1/\kappa + t_c)/(1/\kappa) = 1 + t_c\kappa$, and $\lambda_2 = \lambda_3 = \sqrt{1/\lambda_1}$.

In the sidewalls, we assume that the bending and the stretching deformations are negligible, resulting in $U_h = 0$.

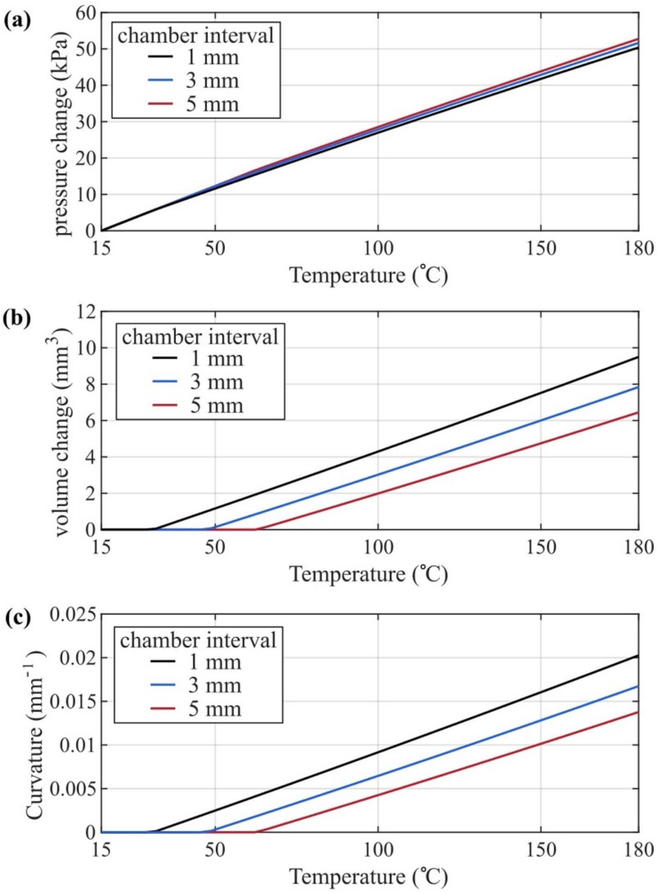

Figure 5. Estimated results from model prediction at the chamber intervals of 1, 3, and 5 mm. (a) Chamber pressure change with respect to the chamber temperature. (b) Chamber volume change with respect to the chamber temperature. (c) Bending curvature of the entire structure with respect to chamber temperature.

The gravitational potential energy U_g depends on the location of the unit segments in H, and then it can be obtained by integration over the total length of the sheet, which is:

$$U_g(\kappa) = \int_{length} \rho g H dl = \frac{\rho g l}{\kappa} - \frac{2\rho g}{\kappa^2} \cdot sin\left(\frac{\kappa l}{2}\right), \quad (7)$$

where ρ is the linear density, including the weight of both the polymer sheet and the cookie dough placed on the sheet, g is the gravitational acceleration, and H is the location of the unit segment in height.

From the principle of the minimum potential energy, the configuration of the sheet at the static equilibrium is derived by solving $d\Pi/d\kappa = 0$:

$$\frac{\mathrm{d}\Pi}{\mathrm{d}\kappa} = N \cdot \left(\frac{\mathrm{d}\left(-\int PdV\right)}{\mathrm{d}\kappa} + \frac{\mathrm{d}U_t}{\mathrm{d}\kappa} + \frac{\mathrm{d}U_b}{\mathrm{d}\kappa}\right) + \frac{\mathrm{d}U_g}{\mathrm{d}\kappa} = 0. \quad (8)$$

Figure 5 presents the estimated results from our model under the design parameters and the test conditions in table 1. As the temperature inside the air chamber increases, both the volume and the pressure of the chamber increase, resulting in an increase in the bending curvature. Also, the curvature at

Table 1. Parameters and test conditions for modeling and experiment.

Parameter	Value	Parameter	Value
l	100 mm	h	15.2 W m^{-2}K^{-1}
x	1, 3, and 5 mm	k	0.261 W m^{-1}K^{-1}
c	1.5 mm	ρ_{air}	1 kg m^{-1}
t_c	5 mm	$\rho_{polymer}$	1180 kg m^{-1}
t_t	2.5 mm	C_{air}	1006 J kg^{-1}K^{-1}
t_b	0.8 mm	$C_{polymer}$	1400 J kg^{-1}K^{-1}
w	25 mm	m_{dough}	10 g
P_0	1 atm	E	1.38 MPa
T_0	15 °C	g	9.81 m s^{-2}
T_{oven}	180 °C		

the target temperature is adjustable according to the chamber interval x. At the temperature of 180 °C, the predicted bending curvatures are 0.0203, 0.0167, and 0.0138 mm^{-1} when the chamber intervals are 1, 3, and 5 mm, respectively. Figures 5(b) and (c) also show that the temperature at which the deformation begins is dependent on the chamber interval. As the chamber interval increases, the total number of the chambers inside the structure decreases, and the linear density of the structure increases. The structure starts to deform at a higher temperature against the gravitational potential energy.

3.4. Heat transfer through conduction

When the cookie mold is placed in a preheated oven, the temperature inside the air chambers gradually increases over time from the room temperature T_0 to the oven temperature T_{oven}. The heat energy is transferred to the polymer sheet through convection in the oven, and the temperature inside the sheet is assumed to be uniform. Then, we approximate the transient behavior of the temperature inside the air chamber using the lumped capacitance method [46], which simply states that the temperature of the object $T(t)$ exponentially progresses toward the temperature of its environment T_{oven},

$$T(t) = T_0 + T_{oven} \cdot \left(1 - e^{(hA_s/\rho VC)\cdot t}\right), \quad (9)$$

where h is the convection coefficient of the air in the oven, A_s is the outer surface area of the sheet, and $\rho VC = (\rho VC)_{polymer} + (\rho VC)_{air}$ is the heat capacity of the sheet which is approximated to the sum of the heat capacity of the polymer and those of the captured air. Figure 6 presents the estimated temperature increase inside the air chamber, which is calculated from the equation (9) and table 1. The sheet with a larger chamber interval shows a less steep slope due to the larger polymer volume increasing its heat capacity.

We also investigated the Biot number $Bi = hl_c/k$ to confirm that the lumped capacitance method is valid for our study, $l_c = V_{polymer}/A_s$ is the characteristic length, and k is the conduction coefficient of the polymer. Under our design parameters and test conditions in table 1, the calculated Biot numbers are 0.11, 0.14, and 0.15 when the corresponding chamber intervals are 1, 3, and 5 mm, respectively. The calculated values are slightly

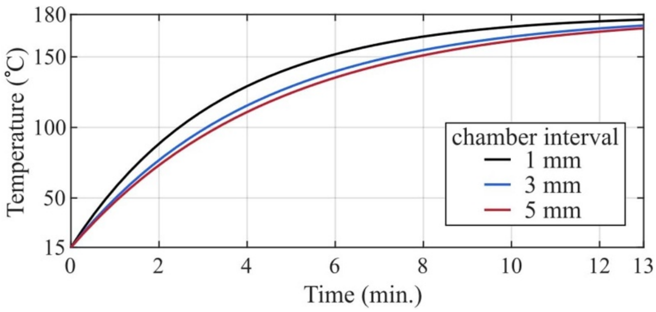

Figure 6. Estimated temperature inside the air chamber over time.

larger than 0.1 but much smaller than 1. Therefore, we used the lumped capacitance method for our study.

4. Experimental evaluation

4.1. Experimental procedure

Figure 7(a) illustrates an experimental setup to validate the analytical model. First, test molds with chamber intervals of 1, 3, and 5 mm were prepared. Three identical molds were prepared for each size. Cookie dough was made of a commercial cookie mix (Gingerbread Cookie Mix, Bread Garden, Inc.) and prepared following the instruction. The cookie dough we used had a viscosity enough to prevent itself from flowing down on a flat mold, so additional guide structures were not necessary to fix the dough on the mold. Cookie dough weighing 10 g was uniformly spread on top of each mold manually. On the front side of the mold, a total of 11 tracking markers were marked at intervals of 10 mm to measure the deformation of the shape. Each mold was then placed in an oven preheated at 180 °C, and the shape transformation of each mold was recorded by a video camera for 13 min. Figure 7(b) shows the trajectories of the tracking markers over time, analyzed by commercial motion tracking software (ProAnalyst, Xcitex). It was repeated for three different chamber intervals (1, 3, and 5 mm) and three identical test molds, as shown in figure 8. Finally, the least square method for circle fitting [47] was applied to the measured locations of the markers, and the changes in curvature were obtained over time.

4.2. Experimental results

The curvatures calculated from the measured tracking markers for 13 min are presented in figure 9(a) for the three test molds with chamber intervals of 1, 3, and 5 mm. The model predictions based on equations (8) and (9) are also plotted in the same figure. In the beginning, there were periods without curvature changes of time during which no curvature change was observed. In other words, the cookie molds did not deform for a while as soon as they were placed in the oven. This period was longer with the sheet of a larger chamber interval. It can be interpreted from our model that the transformation does not occur until the temperature reaches a certain level enough to change the chamber volume against the gravitational energy as mentioned in figures 5(a) and (b). This activation period was long for a large chamber interval, since the gravitational energy to overcome became large and the temperature rose slowly at the same time. It was also noted that the activation time for transformation was slightly longer than that predicted by the model. This seems due to the lumped capacitance assumption that there is no temperature gradient inside the elastomer material. In real experiments, the heat was transmitted gradually from the elastomer surface to the internal air chambers, so the air temperature increased slightly slower than what we expected. The bending curvatures then increased gradually until the molds reached the final curvatures. After 8–10 min, the molds nearly maintained the deformed shapes until the cookies were fully baked. This is because the temperature inside the air chamber reached the oven temperature of 180 °C.

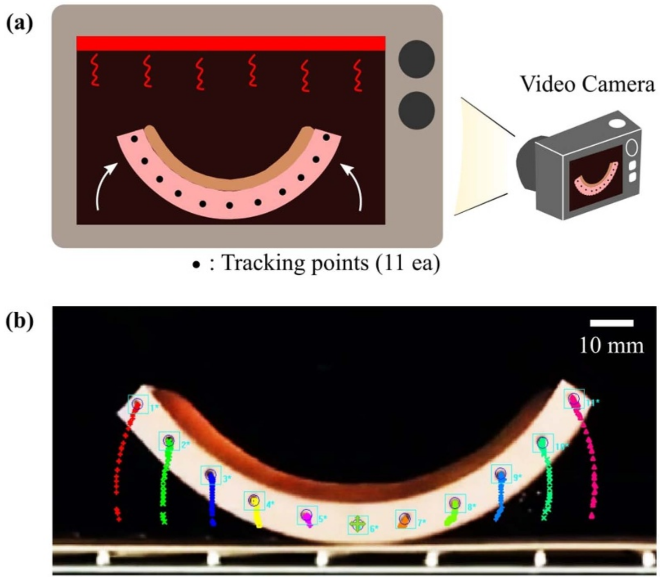

Figure 7. (a) Schematic of the experimental setup used to characterize the cookie mold for a bent shape. (b) A still image of the mold with the trajectories of the tracking points over time extracted from a video clip.

Figure 9(b) shows the relation between the chamber interval and the final bending curvature. The measured final curvatures at 13 min are 0.0188 (SD: 0.0005), 0.0146 (SD: 0.0006), and 0.0109 (SD: 0.0008) mm^{-1} when the chamber intervals are 1, 3, and 5 mm, respectively. The measured final curvature decreased as the chamber interval increased. The result comparisons of the three chamber intervals with their respective analytical models from the equations (8) and (9) are also shown in figures 9(a) and (b). The estimated curvatures at 13 min are 0.0196, 0.0155, and 0.0124 mm^{-1} when the chamber intervals are 1, 3, and 5 mm, respectively. The measured final curvatures showed consistency with the models, but the measured values were slightly smaller than the estimated values from the models. This small discrepancy may be due to several issues, including underestimation of the elastic energy of the structure, stiffness changes of the cookie dough, air leakage of the structure, and the simplified assumptions and models.

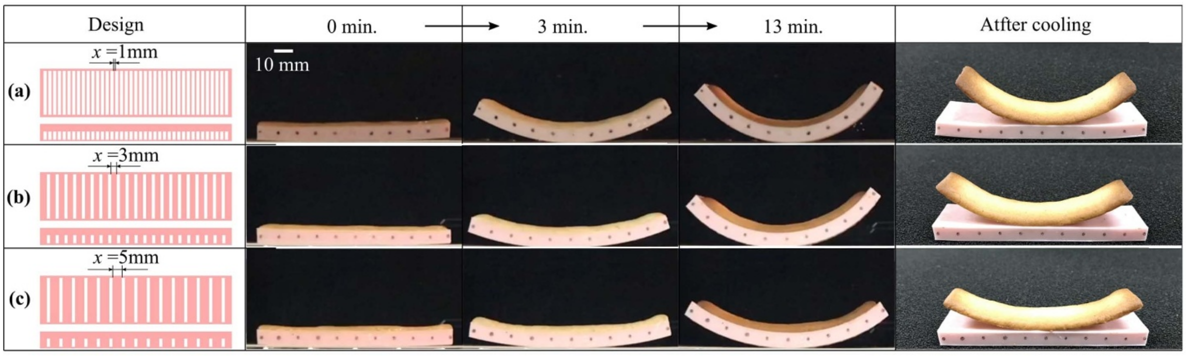

Figure 8. Captured images during experiments. Shape transformation of the test molds from flat dough to bent shapes with a chamber intervals of (a) 1 mm, (b) 3 mm, and (c) 5 mm.

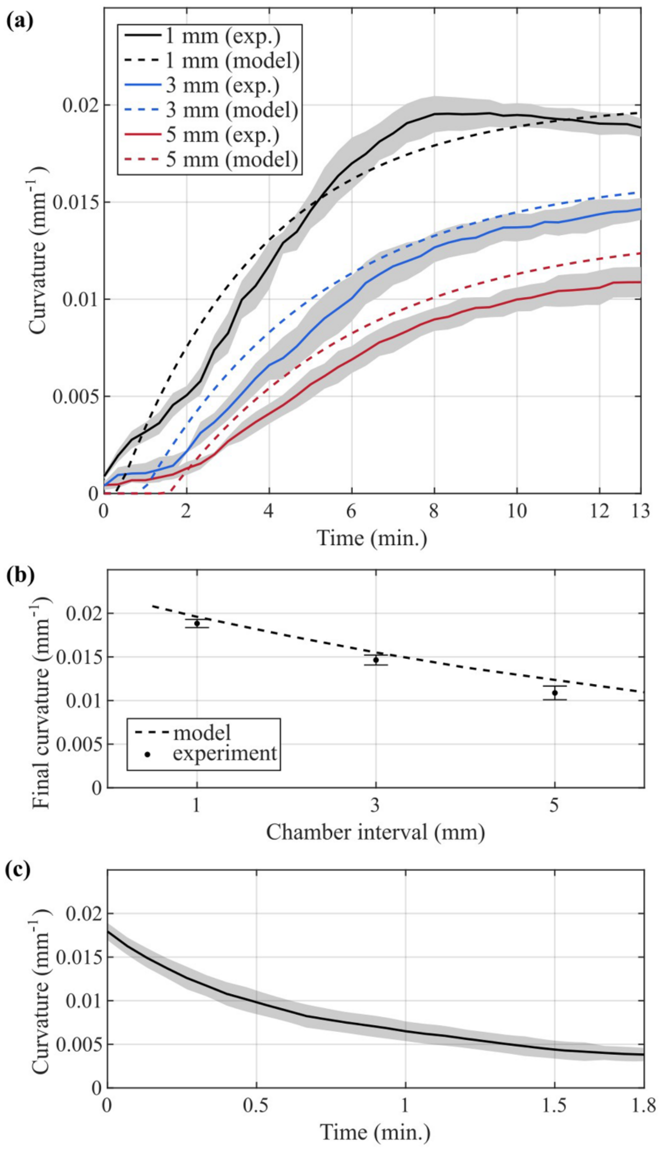

Figure 9. (a) The changes in curvature of the test molds over time. Each experimental curve consists of a mean curve and shaded error bar that spans ± 1 standard deviation. (b) The relation between the chamber interval and the final curvature of the structure. (c) The changes in curvature of the test molds ($x = 1$ mm) during cooling process at the room temperature.

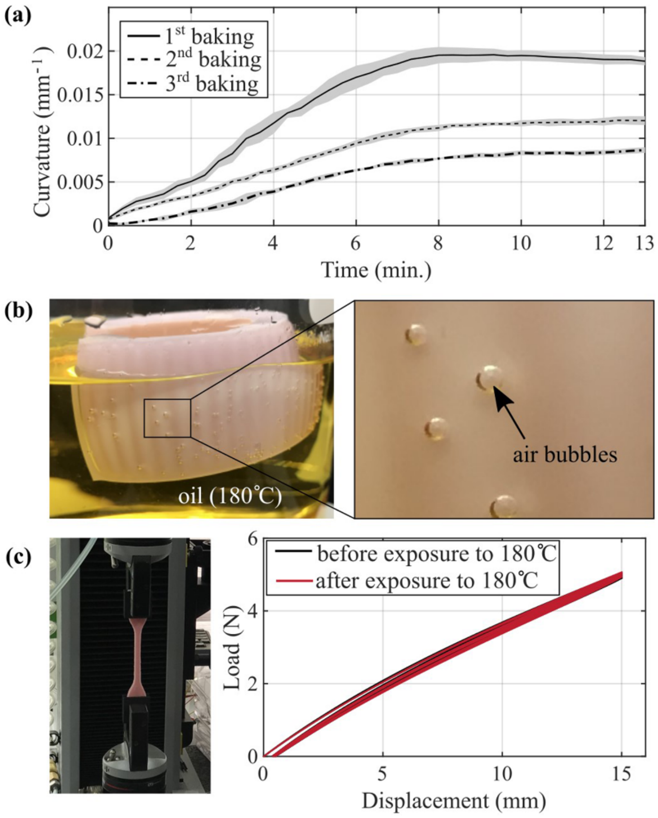

Figure 10. Repeatability test result for the molds with a chamber interval of 1 mm. (a) Changes in curvature over time for three times of baking. Each experimental curve shows a mean curve with a shaded error band of standard deviation. (b) Observed air bubbles on the bottom layer of the mold. (c) Tensile test result of the silicone specimens before and after exposure to 180 °C for 15 min.

When the cookie molds were taken out of the oven and exposed to the room temperature after baking, the curvature of the cookie mold decreased without any delay and returned to the initial flat shape, as shown in figure 9(c). The returning process can be further accelerated by active cooling with cold air or water.

We also performed repeatability tests using three identical test molds with a chamber interval of 1 mm. During the three repeated tests, decreases in the final curvature were observed, as shown in figure 10(a). This decrease was linked to the high air permeability of the silicone elastomer since we observed air bubbles on the thin bottom layer when we put the structure in preheated oil of 180 °C, as shown in figure 10(b). The failure in bonding of the top and the bottom layers during fabrication may lead to air leakage. However, during the airtight test, we did not observe air bubbles at the seams, and we concluded that the air leakage was mainly due to the high permeability of the silicone material itself. It can be also attributed to the thermal degradation of the silicone material at high temperatures related to the chain scission of the polymer bonds which may increase the gas permeability of the structure.

We also performed an experiment to examine whether the change in the modulus of the elastomer occurred with exposure to the temperature of 180 °C. The tensile tests were carried out and repeated with three identical specimens before and after exposure to 180 °C for 15 min. As shown in figure 10(c), the change of the modulus was not observed.

As result of the above experiments, we believe that the performance degradation during repeated uses is mainly due to air leakage of the silicone material we used. Therefore, further investigation is required to find more airtight materials and methods of sealing the air chamber while maintaining similar elasticity.

5. Self-folding in 3D shapes

5.1. Designs with various chamber arrangements

In the previous sections, we modeled and characterized the response of the proposed self-folding structure for transformation into the curved arc. We explore designs with various chamber arrangements allowing more complex shape transformations in this section, as shown in figure 11, which is beneficial in that they provide many options to a designer for creating more realistic 3D shapes by adjusting the design parameters.

Molds with diagonal air chambers provide both bending and twisting functions, as shown in figure 11(a). Depending on the chamber angle θ, the molds show different ratios of the bending and the twisting angles. Figure 12(a) shows the measured bending and twisting angles of the baked cookies. Increase of the chamber angle decreases the bending angle while increasing the twisting angle. The ratios of the bending and twisting angles at the chamber angles of 15°, 30°, and 45° were 2.2, 1.2, and 0.4, respectively. The ratio decreased with increase of the chamber angles.

Furthermore, we were able to achieve more complex shapes by combining different chamber patterns. Figure 11(b) shows a mold with a 3-mm air chamber interval for the left half and 1 mm interval for the right half. Due to the different chamber intervals, the sheet deformed with two different curvatures; the curvature of the left side is smaller than that of the right side. In this way, it is possible to continuously change the bending curvature by gradually varying the intervals of the air chambers. Figure 11(c) shows another design for pure bending on the left side combined with bending and twisting on the right side through partially diagonal chamber patterns. Lastly, figure 11(d) shows a bidirectional folding with opposite directions of curvatures, which is called *s*-bending. In this design, the top layer is thicker than the bottom layer on the left side, while the right side is in the other way. It allows the sheet to have the strain-limiting layers on the top for the left side and on the bottom for the right side, resulting in *s*-shaped transformation. A simple way of fabricating the *s*-bending cookie mold is to make a mold with a for pure bending first, cut it into halves, flip one piece over, and then bond the two pieces again. It makes the air chambers on the left and right sides biased towards the bottom and the top, respectively.

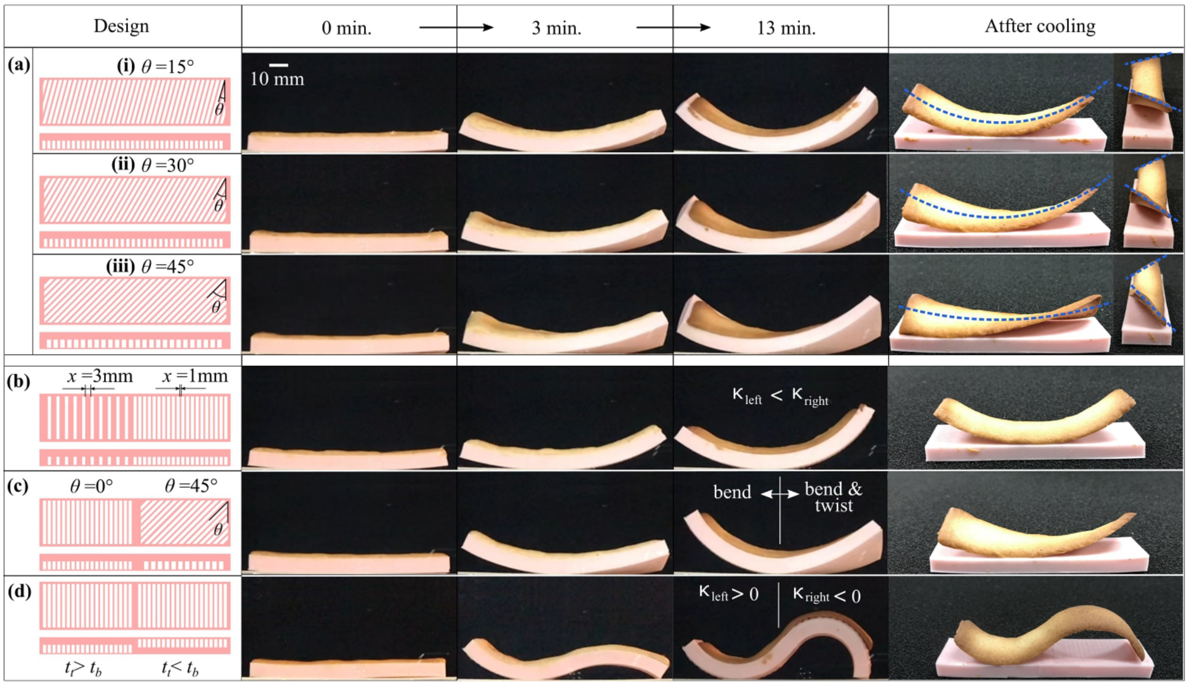

Figure 11. Designs with various chamber arrangements: (a) bending and twisting, (b) partially different bending curvature, (c) bending and partial twisting, and (d) s-curve bending.

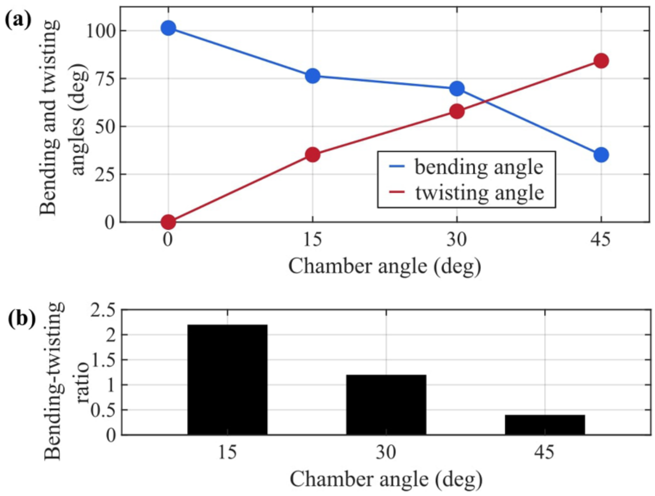

Figure 12. Experimental results of the cookie mold designs with diagonal air chamber patterns. (a) Changes in the bending and the twisting angles with respect to the chamber angles. (b) Changes in the ratio of the bending and the twisting angles with respect to the chamber angle.

5.2. Practical prototypes of pop-up cookie molds

As more practical applications, we demonstrate several prototypes with more complex shapes for attraction. Figure 13(a) shows flower-shaped cookie molds with different configurations of the petals. In the initial states, they are all flat so that the users can easily place cookie dough on the molds. However, they deform differently during baking due to the different arrangements of the air chambers inside the molds: (a) bending, (b) bending-twisting, and (c) *s*-bending.

More complex designs can be also achieved by placing several transformable parts on the same mold. Figure 13(b) is a mold for a cookie with a shape of an octopus. The design includes various chamber pattern in a single mold to express the 3D shape of an octopus. In this case, the head and the legs can be naturally transformed in different directions. Figure 13(c) is another prototype that contains multiple objects: a flower and a butterfly. In this design, bending-twisting for the petals, bending and *s*-bending for the leaves, and pure bending for the butterfly were employed. The prototypes we demonstrated are no more than a few examples of the proposed self-folding molds. More interesting and attractive designs can be created based on the designer's imagination and creativity.

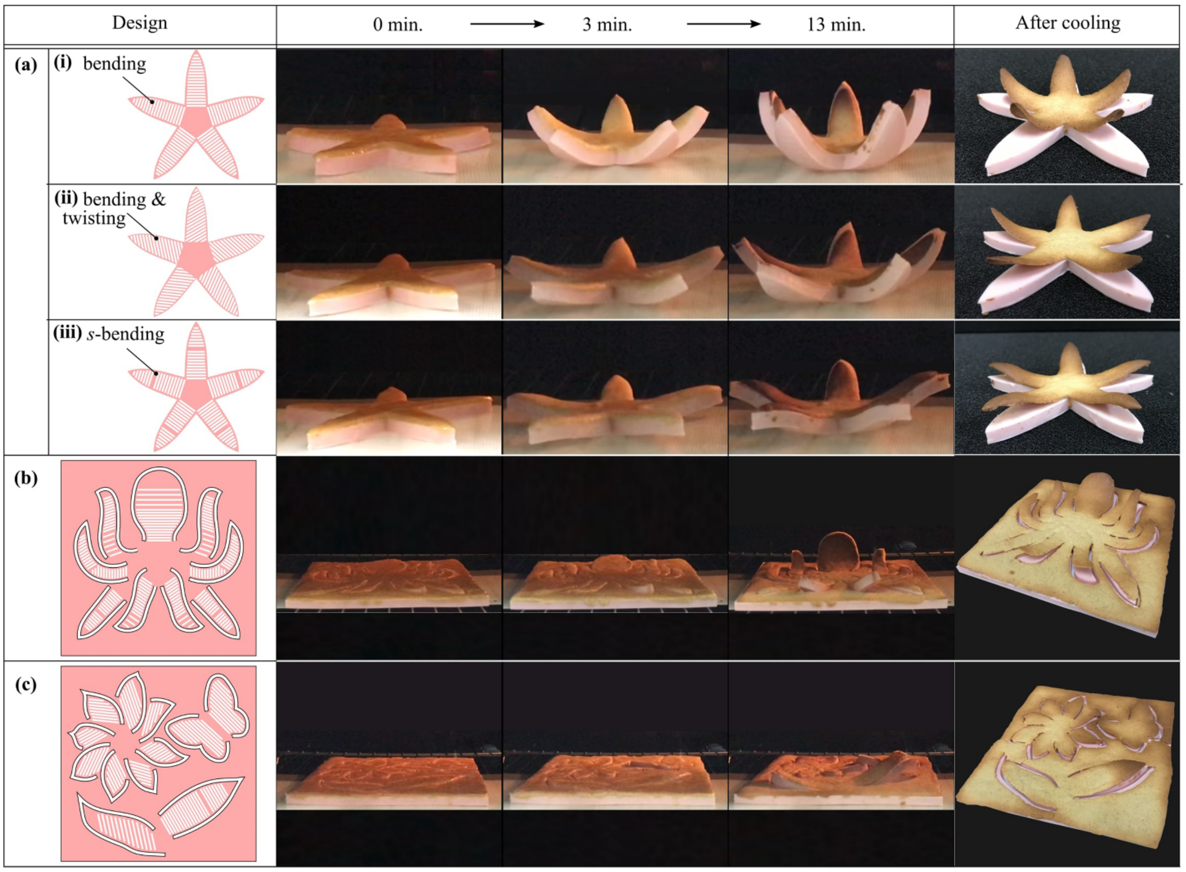

Figure 13. Practical prototypes of pop-up cookie molds. (a) Different flower shapes with chamber arrangements of (i) bending, (ii) bending-twisting, and (iii) *s*-banding. (b) Octopus. (c) Flower and butterfly.

6. Conclusion

This study proposed a mechanism of self-folding polymer structures that can be transformed from flat shapes to pre-programmed 3D shapes. While previous studies have realized the self-folding function using special materials, such as SMA, SMP, and liquid crystal elastomer, we developed a simple method that used thermal expansion of the embedded air chamber array. During the folding process, the structure enables shape changes the object placed on it. Using the proposed design, we developed pop-up cookie molds that allowed for baking of 3D-shaped cookies without special techniques.

We first developed analytical models and then experimentally validated the models to determine the critical parameters to and their effects on the performance of the structure's shape transformation. Based on the agreement between the model predictions and the experimental results, we confirmed that this study can provide design guidelines for the proposed pop-up cookie molds. In addition to basic deformation, such as simple bending, we also tested more complex shape transformations based on combinations of different air chamber patterns, such as bending-twisting, curvature change, bending-partial twisting, and *s*-bending were also experimentally characterized. The results allowed us to estimate proper design parameters and to arrange the patterns of the embedded air chambers to achieve desired 3D shapes.

However, further investigation is still required to predict various shape deformations, since the analytical models developed in this study are based on the simplified geometric assumptions and theories. For better control of the mold structures over time, we also need to adjust the heat capacity of the structure by coating it with a heat-resistant material with a controlled thickness to slow down the process of heat transfer into the embedded air chambers. It would be also useful to examine the hardness change of the cookie dough during baking to find the optimal deformation time within the recommended the baking time.

Another limitation is that the performance of the proposed self-folding structures degraded during the repeated uses, which was mainly due to the change of the air permeability of the silicone elastomer. We are currently investigating different methods of eliminating or reducing this effect for consistency in the performance for multiple uses. One possible approach is use of fluoroelastomer that has low air permeability and high-temperature resistance [48]. Mixing nanoparticles in polymer materials [49] or surface coating with low permeability materials [50] could be an other alternative.

It is also important to consider other physical behaviors that can affect the behavior of the structure over time. For example, water evaporation from the cookie dough during baking causes weight loss of approximately 15%, which may affect the final curvature of the sheet. We can address this issue by improving the analytical models that include weight reduction terms due to the evaporation. Another effect of evaporation may be cooling of the cookie mold, which may slow down the start of deformation, as discussed in figure 9(a), which is also an area of future work. Multi-physics simulation, such as finite element analysis, considering fluid-structure interaction and heat transfer, would be an option to improve the prediction accuracy.

Another area of future work would be addition of self-assembly functions using pop-up folding, as demonstrated in manufacturing of microrobots [51, 52], to realize even more complex and attractive structures. We can also further simplify the fabrication process by using a commercially available closed-cell silicone foam (i.e. sponge) with an additional non-porous layer of silicone laminated onto one side [53].

The proposed structures are made of a single polymer material, designed and fabricated in various shapes in a preprogrammed manner. It will be beneficial for the factory to produce large quantities of complex shapes. The pop-up cookie molds will provide a delightful experience for children who will have fun of making cookies at home. We believe that our research would provide a new research direction and an opportunity to broaden the application areas of soft robotics and smart materials and structures.

Data availability statement

All data that support the findings of this study are included within the article (and any supplementary files).

Acknowledgment

This work was supported by the National Research Foundation (NRF) Grant (No. NRF-2016R1A5A1938472) funded by the Korean Government (MSIT).

ORCID iDs

Junghan Kwon https://orcid.org/0000-0002-4315-235X
Yong-Lae Park https://orcid.org/0000-0002-2491-2114

References

[1] Sorensen L B, Moller P, Flint A, Martens M and Raben A 2003 Effect of sensory perception of foods on appetite and food intake: a review of studies on humans *Int. J. Obesity* **27** 1152
[2] Spence C, Okajima K, Cheok A D, Petit O and Michel C 2016 Eating with our eyes: from visual hunger to digital satiation *Brain Cognit.* **110** 53–63
[3] Bollini M, Barry J and Rus D 2011 Bakebot: baking cookies with the pr2 *The PR2 Workshop: Results, Challenges and Lessons Learned in Advancing Robots With a Common Platform, IROS*
[4] Lipton J I, Cutler M, Nigl F, Cohen D and Lipson H 2015 Additive manufacturing for the food industry *Trends Food Sci. Technol.* **43** 114–23
[5] Dankar I, Haddarah A, Omar F E L, Sepulcre F and Pujolà M 2018 3D printing technology: the new era for food customization and elaboration *Trends Food Sci. Technol.* **75** 231–42
[6] Lipton J, Arnold D, Nigl F, Lopez N, Cohen D L, Norén N and Lipson H 2010 Multi-material food printing with complex internal structure suitable for conventional post-processing *Solid Freeform Symp.* pp 809–15
[7] Sun J, Zhou W, Huang D, Fuh J Y H and Hong G S 2015 An overview of 3D printing technologies for food fabrication *Food Bioprocess Technol.* **8** 1605–15
[8] Sun J, Zhou W, Yan L, Huang D and Lin L 2018 Extrusion-based food printing for digitalized food design and nutrition control *J. Food Eng.* **220** 1–11
[9] de Marco C, Pané S and Nelson B J 2018 4D printing and robotics *Sci. Robot.* **3** eaau0449
[10] Yang G-Z, Fischer P and Nelson B 2017 New materials for next-generation robots *Sci. Robot.* **2** eaau0448
[11] Tibbits S 2014 4D printing: multi-material shape change *Archit. Des.* **84** 116–21
[12] Gladman A S, Matsumoto E A, Nuzzo R G, Mahadevan L and Lewis J A 2016 Biomimetic 4D printing *Nat. Mater.* **15** 413
[13] Wang W, Yao L, Zhang T, Cheng C-Y, Levine D and Ishii H 2017 Transformative appetite: shape-changing food transforms from 2D to 3D by water interaction through cooking *Proc. 2017 Conf. on Human Factors in Computing Systems* (ACM) pp 6123–32
[14] Ilievski F, Mazzeo A D, Shepherd R F, Chen X and Whitesides G M 2011 Soft robotics for chemists *Angew. Chem.* **123** 1930–5
[15] Jang S-H, Na S-H and Park Y-L 2017 Magnetically assisted bilayer composites for soft bending actuators *Materials* **10** 646
[16] Park M, Ohm Y, Kim D and Park Y-L 2019 Multi-material soft strain sensors with high gauge factors for proprioceptive sensing of soft bending actuators *2019 2nd IEEE Int. Conf. Soft Robotics (RoboSoft)* (IEEE) pp 384–90
[17] Wirekoh J, Parody N, Riviere C N and Park Y-L 2020 Design of fiber-reinforced soft bending pneumatic artificial muscles for wearable tremor suppression devices *Smart Mater. Struct.* **30** 015013
[18] Jung J, Park M, Kim D and Park Y-L 2020 Optically sensorized elastomer air chamber for proprioceptive sensing of soft pneumatic actuators *IEEE Robot. Autom. Lett.* **5** 2333–40
[19] Hong T H, Park S-H, Park J-H, Paik N-J and Park Y-L 2020 Design of pneumatic origami muscle actuators (pomas) for a soft robotic hand orthosis for grasping assistance *2020 3rd IEEE Int. Conf. Soft Robotics (RoboSoft)* (IEEE) pp 627–32
[20] Stoychev G, Puretskiy N and Ionov L 2011 Self-folding all-polymer thermoresponsive microcapsules *Soft Matter* **7** 3277–9
[21] Raviv D *et al* 2014 Active printed materials for complex self-evolving deformations *Sci. Rep.* **4** 7422
[22] An B, Miyashita S, Tolley M T, Aukes D M, Meeker L, Demaine E D, Demaine M L, Wood R J and Rus D 2014 An end-to-end approach to making self-folded 3D surface shapes by uniform heating *2014 IEEE Int. Conf. Robotics and Automation (ICRA)* (IEEE) pp 1466–73
[23] Felton S, Tolley M T, Demaine E, Rus D and Wood R J 2014 A method for building self-folding machines *Science* **345** 644–6
[24] Tolley M T, Felton S M, Miyashita S, Aukes D, Rus D and Wood R J 2014 Self-folding origami: shape memory composites activated by uniform heating *Smart Mater. Struct.* **23** 094006
[25] Zhang Q, Zhang K and Hu G 2016 Smart three-dimensional lightweight structure triggered from a thin composite sheet via 3D printing technique *Sci. Rep.* **6** 22431

[26] Ding Z, Yuan C, Peng X, Wang T, Qi H J and Dunn M L 2017 Direct 4D printing via active composite materials *Sci. Adv.* **3** e1602890
[27] An B *et al* 2018 Thermorph: democratizing 4D printing of self-folding materials and interfaces *Proc. 2018 Conf. Human Factors in Computing Systems* (ACM) 260
[28] Wang G, Yang H, Yan Z, Gecer Ulu N, Tao Y, Gu J, Kara L B and Yao L 2018 4DMesh: 4D printing morphing non-developable mesh surfaces *31st Annual Symp. User Interface Software and Technology* (ACM) pp 623–35
[29] Kotikian A, McMahan C, Davidson E C, Muhammad J M, Weeks R D, Daraio C and Lewis J A 2019 Untethered soft robotic matter with passive control of shape morphing and propulsion *Sci. Robot.* **4** eaax7044
[30] Liu Y, Boyles J K, Genzer J and Dickey M D 2012 Self-folding of polymer sheets using local light absorption *Soft Matter* **8** 1764–9
[31] Liu Y, Shaw B, Dickey M D and Genzer J 2017 Sequential self-folding of polymer sheets *Sci. Adv.* **3** e1602417
[32] Plucinsky P, Kowalski B A, White T J and Bhattacharya K 2018 Patterning nonisometric origami in nematic elastomer sheets *Soft Matter* **14** 3127–34
[33] Zeng H, Wani O M, Wasylczyk P and Priimagi A 2018 Light-driven, caterpillar-inspired miniature inching robot *Macromol. Rapid Commun.* **39** 1700224
[34] Kim Y, Yuk H, Zhao R, Chester S A and Zhao X 2018 Printing ferromagnetic domains for untethered fast-transforming soft materials *Nature* **558** 274
[35] Kim Y, Parada G A, Liu S and Zhao X 2019 Ferromagnetic soft continuum robots *Sci. Robot.* **4** eaax7329
[36] Bartlett N W, Tolley M T, Overvelde J T B, Weaver J C, Mosadegh B, Bertoldi K, Whitesides G M and Wood R J 2015 A 3D-printed functionally graded soft robot powered by combustion *Science* **349** 161–5
[37] Wehner M, Truby R L, Fitzgerald D J, Mosadegh B, Whitesides G M, Lewis J A and Wood R J 2016 An integrated design and fabrication strategy for entirely soft, autonomous robots *Nature* **536** 451
[38] Peraza-Hernandez E, Hartl D and Lagoudas D 2013 Shape memory alloy laminate for design of self-folding reconfigurable structures *19th Int. Conf. Composite Materials*
[39] Rodrigue H, Wang W, Bhandari B, Han M-W and Ahn S-H 2014 Cross-shaped twisting structure using SMA-based smart soft composite *Int. J. Precis. Eng. Manuf.-Green Technol.* **1** 153–6
[40] Cengel Y A and Boles M A 2007 *Thermodynamics: An Engineering Approach 6th Edition* (New York: The McGraw-Hill Companies, Inc.)
[41] Shepherd R F, Ilievski F, Choi W, Morin A, Stokes A A, Mazzeo A D, Chen X, Wang M and Whitesides G M 2011 Multigait soft robot *Proc. Natl Acad. Sci.* **108** 20400–3
[42] Park Y-L, Chen B-R and Wood R J 2012 Design and fabrication of soft artificial skin using embedded microchannels and liquid conductors *IEEE Sens. J.* **12** 2711–18
[43] Vogt D M, Park Y-L and Wood R J 2013 Design and characterization of a soft multi-axis force sensor using embedded microfluidic channels *IEEE Sens. J.* **13** 4056–64
[44] Majidi C, Shepherd R F, Kramer R K, Whitesides G M and Wood R J 2013 Influence of surface traction on soft robot undulation *Int. J. Robot. Res.* **32** 1577–84
[45] Paoletti P, Jones G W and Mahadevan L 2017 Grasping with a soft glove: intrinsic impedance control in pneumatic actuators *J. R. Soc. Interface* **14** 20160867
[46] Bergman T L, Incropera F P, DeWitt D P and Lavine A S 2011 *Fundamentals of Heat and Mass Transfer* (New York: Wiley)
[47] Pratt V 1987 Direct least-squares fitting of algebraic surfaces *ACM SIGGRAPH Comput. Graph.* **21** 145–52
[48] Sharma G, Klintberg L and Hjort K 2011 Viton-based fluoroelastomer microfluidics *J. Micromech. Microeng.* **21** 025016
[49] Zhou H, Wang H, Niu H, Gestos A, Wang X and Lin T 2012 Fluoroalkyl silane modified silicone rubber/nanoparticle composite: a super durable robust superhydrophobic fabric coating *Adv. Mater.* **24** 2409–12
[50] Zhu H, Dai Z and Tu W 2017 Study on the preparation and performance of low gas permeability trifluoropropyl phenyl silicone rubber *RSC Adv.* **7** 39739–47
[51] Whitney J P, Sreetharan P S, Ma K Y and Wood R J 2011 Pop-up book MEMS *J. Micromech. Microeng.* **21** 115021
[52] Sreetharan P S, Whitney J P, Strauss M D and Wood R J 2012 Monolothic fabrication of milimeter-scale machines *J. Micromech. Microeng.* **22** 055027
[53] Robertson M A and Paik J 2017 New soft robots really suck: vacuum-powered systems empower diverse capabilities *Sci. Robot.* **2** eaan6357